Zinc oxide hexagram whiskers

Xu, Chunxiang; Sun, Xiaowei; Dong, Zhili; Zhu, Guangping; Cui, Yiping

2006

Xu, C. X., Sun, X., Dong, Z. L., Zhu, G. P. & Cui, Y. P. (2006). Zinc oxide hexagram whiskers. Applied Physics Letters, 88(9).

https://hdl.handle.net/10356/93776

https://doi.org/10.1063/1.2179133

Zinc oxide hexagram whiskers

C. X. Xu and X. W. Sun[a)]
School of Electric and Electronic Engineering, Nanyang Technological University, Nanyang Avenue, Singapore 639798 and Department of Electronic Engineering, Southeast University, Nanjing 210096, People's Republic of China

Z. L. Dong
School of Materials Science and Engineering, Nanyang Technological University, Nanyang Avenue, Singapore 639798

G. P. Zhu and Y. P. Cui
Department of Electronic Engineering, Southeast University, Nanjing 210096, People's Republic of China

(Received 30 August 2005; accepted 4 January 2006; published online 27 February 2006)

Through vapor-phase transport method, zinc oxide hexagram whiskers with uniform size and morphology were fabricated by heating a mixture source of zinc oxide, indium oxide, and graphite powders in air. Each whisker presented a hexagonal disk core closed by six equivalent surfaces of $\{10\bar{1}0\}$ and was surrounded by side nanorods grown along the diagonal of the core disk in the 6-symmetric directions of $\pm[11\bar{2}0]$, $\pm[2\bar{1}\bar{1}0]$, and $\pm[1\bar{2}10]$. Based on the vapor-liquid-solid mechanism, the growth process of the zinc oxide hexagrams were discussed by considering the thermal dynamic properties of zinc oxide and indium oxide. © *2006 American Institute of Physics*. [DOI: 10.1063/1.2179133]

Zinc oxide (ZnO), a traditional oxide semiconductor has attracted great interest because of its unique properties and multifunctional applications in recent years. It has a direct wide band gap of 3.34 eV and a strong excitonic binding energy of 60 meV at room temperature. These properties demonstrate that it should be a good candidate for UV light-emitting diodes and laser diodes with high efficiency and low threshold. Besides the optical properties, nano/microstructures of ZnO have also been paid considerable attention because of its aesthetic morphologies and the attractive promising potential in nanodevices, such as nanolasers and nanosensors. So far, approaches have been applied to obtain various nanostructural ZnO, which included one-dimensional (1D) nanowires,[1] nanorod,[2] nanoneedles,[3] nanopins,[4] nanopencils,[5] and nanotubes,[6] and two-dimensional (2D) nanobelts,[7] nanocombs,[8] and nanodisks,[9] and three-dimensional (3D) tetrapods,[10] nanorings,[11] hierarchical,[12] and network.[13] The diversities of the ZnO crystal morphology imply its multifunctional applications in electronics, photonics, even bioelectronics areas. For this consideration, controlling the growth process and exploring novel structures of ZnO are important in understanding the crystal growth mechanism and to further develop new functional devices.

Generally, ZnO favors a wurtzite lattice structure. The most common among the revealed rich nanostructures grows along the [0001] direction to form the 1D structure. The combination of the three sets of fast growth directions, $\langle 11\bar{2}0\rangle$, $\langle 10\bar{1}0\rangle$, and [0001], and the three area-adjustable facets $\{11\bar{2}0\}$, $\{10\bar{1}0\}$, and {0001} of ZnO results in a diverse group of hierachical nanostructures.[12,14,15] To obtain unusual nanostructures, fast growth directions have to be suppressed. Two research groups employed citrate anions as a structure-directing agent[16] and anionic bis(2-ethylhexyl) sulfosuccinate (AOT) as a molecular template[17] to suppress ZnO growing along the [0001] direction and to induce the formation of a disk shaped. Recently, we reported hexagonal ZnO nanodisks,[18] which grew along the 6-symmetic $\langle 10\bar{1}0\rangle$ directions, fabricated by a vapor-phase transport (VPT) method. In this paper, we shall present starlike ZnO whiskers (hexagrams) based on our previous work and analyze the formation mechanism.

The ZnO hexagram whiskers were produced on a silicon stripe through the VPT approach. The source material was a mixture of ZnO, indium oxide (In_2O_3), and graphite powders with a mole ratio of 1:0.2:4. The source and substrate temperatures were kept at 1100 °C and 750 °C, respectively. A white layer of product was deposited on the substrate after sintering for 45 min in air.

A JEOL scanning electron microscopy (SEM) was employed to examine the morphology and the energy dispersive x-ray spectroscopy (EDX) of the product. Based on the EDX measurement, the spatial distribution of Zn, O, and In is analyzed by the element mapping technique. The crystal structure of the sample was characterized by x-ray diffraction (XRD) using the copper $K\alpha$ line under an accelerating voltage of 40 kV. A JEOL 2010 transmission electron microscope (TEM) operated at 200 kV was employed to detect the selected area electron diffraction (SAED) pattern.

Figure 1 shows the SEM images of the product with low (a), medial (b), and high [(c) and (d)] magnifications. It can be seen, from Fig. 1(a), that the ZnO whiskers present a starlike morphology with six symmetric antennae, we call hexagrams. All the hexagrams are uniform in dimension. From the enlarged SEM image in Fig. 1(b), it is clearly seen that a hexagonal disk with about 2 μm in diagonal is inlaid at the center of 6-symmetric nanorod arrays. It is noted in Figs. 1(b) and 1(c) that the side nanorods extend outward from the six corners along the diagonal of the disk to form six bundles of branches with a diameter of about 1 μm. The

[a)]Author to whom correspondence should be addressed; electronic mail: exwsun@ntu.edu.sg

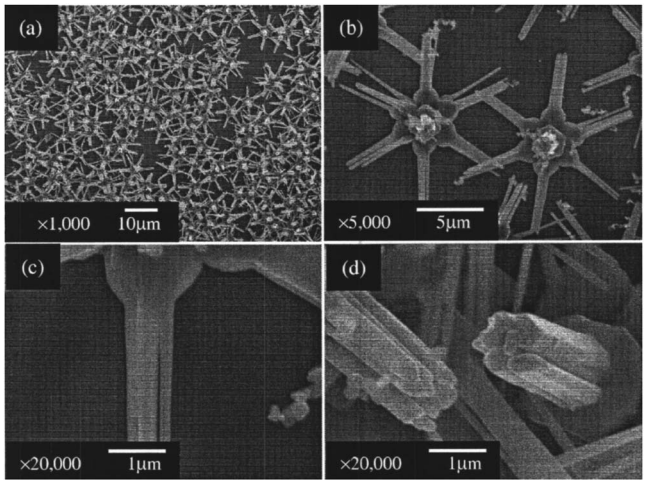

FIG. 1. SEM images of ZnO hexagram whiskers (a) with enlarged two hexagrams (b), enlarged side rods (c) and enlarged center rod array (d).

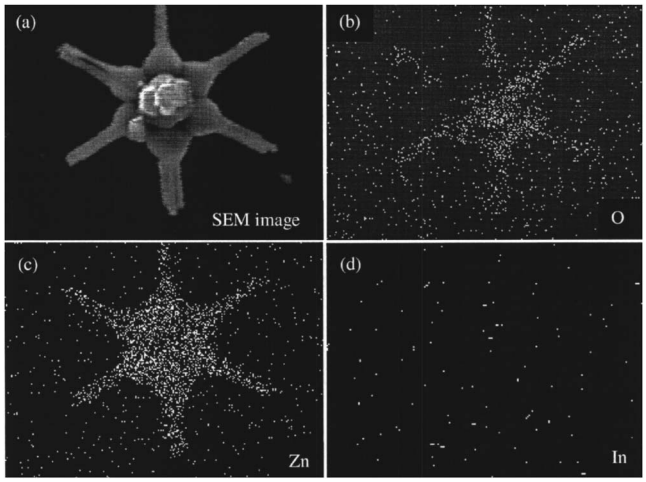

FIG. 3. SEM image (a) of an individual hexagram of ZnO and the corresponding element mappings of O (b), Zn (c) and In (d), respectively.

side nanorods making up the bundles are about 5 μm in length and 250 nm in diameter, with a big base attached on the angles of the disk. There is a bundle of nanorods with about 1 μm in length and 250 nm in diameter standing vertically on each disk surface [Fig. 1(d)].

Figure 2 shows the XRD pattern of the hexagrams. As indexed in the spectrum, all diffraction peaks match the hexagonal structure of wurtzite ZnO. It is noted that no obvious diffraction signal from the indium compound was observed, although there was about 20 at. % In_2O_3 mixed into the source. The EDX spectrum of the sample, detected over a large area [Fig. 1(a)], is shown as the insert in Fig. 2, to analyze the element content in the hexagrams. Indium signal is hardly observed in the EDX spectrum, although the calculated content of In is about 1 at. %. The results of XRD and EDX indicates that only a small amount of indium is doped into the lattice sites of ZnO. This phenomenon is understood by comparing the thermal dynamic properties of In_2O_3 and ZnO. The bond enthalpies of Zn–O and In–O in gaseous diatomic species are 159 ± 4 kJ/mol and 320.1 ± 41.8 l kJ/mol, respectively, and the calculated lattice energies of ZnO and In_2O_3 are 4142 kJ/mol and 13928 kJ/mol,[19] respectively. These parameters imply that In_2O_3 is more difficult to be reduced into In vapor compared to ZnO being reduced into Zn, and the reduced Zn vapor is easier to bind with oxygen than In vapor.

The mixture of ZnO and In_2O_3 has been used to synthesize 3D hierarchical ZnO nanostructures by Lao *et al.*[12] In their experiment, the hexagonal In_2O_3 cores were formed first, and the secondary ZnO nanorods grew along the [0001] direction from the side surface of In_2O_3 to form a heteronanostructure with sixfold symmetry in multiple rows. Similarly, Gao and Wang[14,15] have also employed the mixture of ZnO and SnO_2 to synthesize 3D ZnO nanopropellers, which were found by first growing a hexagonal ZnO core along the [0001] direction and enclosed by $\{2\bar{1}\bar{1}0\}$ surfaces, and later formed multilayer nanoblades along the sixfold symmetric equivalent directions of $\langle 2\bar{1}\bar{1}0\rangle$ perpendicular to the core. In the present case, the hexagrams are homogeneously composed of ZnO and the core and side branches distribute almost on the same plane to form a quasi-2D structure due to the growth suppression in the [0001] direction. Figure 3 shows the element mappings of an individual whisker measured by EDX. It can be seen that Zn and O are homogeneously distributed on the corresponding SEM image area of the hexagram. Only sparse dots appear randomly on the indium map, which is not enough to confirm the existence of indium. In order to understand the growth directions of the hexagram whiskers, SAED patterns were taken, respectively, from the edges of the core disk and the side rods by TEM, as shown in Fig. 4. The core disk presents clear hexagonal dif-

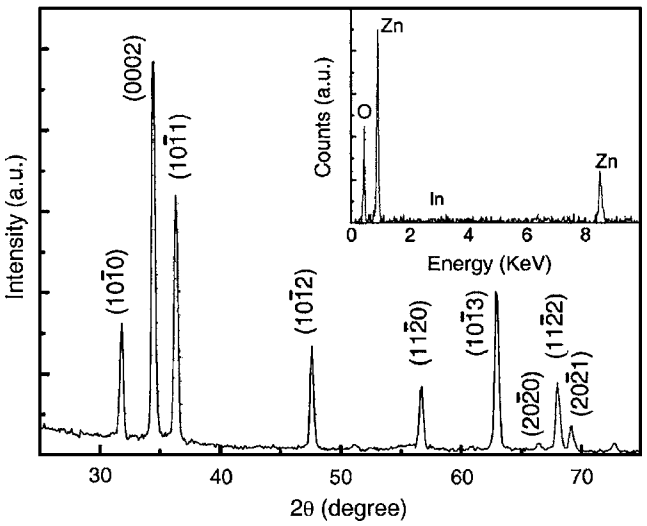

FIG. 2. XRD pattern of ZnO hexagram whisker, inserted by the EDX spectrum.

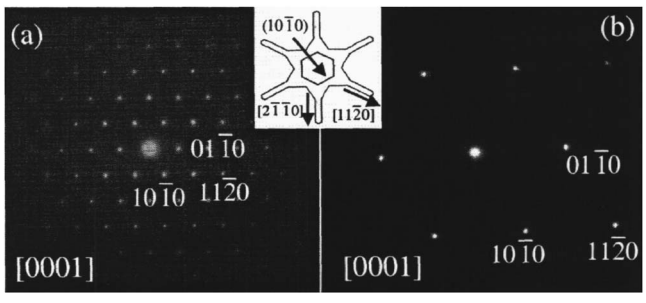

FIG. 4. SAED pattern taken from the edge of the core disk (a) and the side nanorod (b) of a ZnO hexagram from the [0001] zone axis. The insert shows schematically the crystallographic planes and directions of the core disk and side nanorods.

fraction spots in Fig. 4(a), which is similar to our previous reported nanodisks.[18] It demonstrates that the core disk is closed by the side surfaces of $(10\bar{1}0)$ and its other five equivalent facets. The side branches have the same SAED patterns [Fig. 4(b)] with the core area and they extended along the diagonal of the disk. It is worth mentioning that the SAED patterns in Figs. 4(a) and 4(b) were obtained without tilting the sample. Thus, it is believed that they grow along the 6-symmetric directions of $\pm[11\bar{2}0]$, $\pm[2\bar{1}\bar{1}0]$, and $\pm[1\bar{2}10]$. The crystallographic planes and the growth directions of the core disk and the side branches are clearly indicated in the inserted schematic diagram between Figs. 4(a) and 4(b).

Based on the well-known vapor-liquid solid (VLS) mechanism, ZnO crystals grow generally along the [0001] direction to form nanowires and nanorods because of the lowest surface energy of the (0002) facet.[20,21] The growth velocity along the [0001] direction can be suppressed in the presence high pressure Zn vapor.[18,22] For example, when the normal source of ZnO or graphite powders were used instead of ZnO nanoparticles or carbon nanotubes, higher vapor pressure was generated and the diameter of the legs of tetrapod ZnO increased with the distance from the core of the whisker, as reported by Leung *et al.*[23] The Zn and ZnO nanodisks,[18,23] ZnO nanonails,[24] and SnO nanodisks[25] were also fabricated in similar conditions. The In_2O_3 in our experiment might play an important role although the exact mechanism is not clear yet. We suspect that In acts as a catalyst to generate higher pressure of Zn vapor and further beneficial to suppress the growth of ZnO along the [0001] direction. In this case, a hexagonal disklike nucleus formed. In the *c* plane, the growth velocity in $\langle 11\bar{2}0\rangle$ is faster than any other direction because of the lower bind energy.[20,21] In the initial growth stage, the incoming Zn vapor was so high that the core disk grew up and bigger bases formed at the side corners of the disk. Gradually, the incoming Zn vapor is reduced due to the consumption of source materials, and the side branches became thinner, forming side antennae. Meanwhile, some vapor condensed on the (0001) surface of the core disk to grow short nanorods along the [0001] direction.

In summary, the ZnO hexagram whiskers were fabricated by adding additional In_2O_3 into the typical mixture source of ZnO and graphite powders. A hexagonal disk core was formed at high vapor pressure and subsequently surrounded by the side branches grown along the 6-symmetric directions of $\langle 11\bar{2}0\rangle$. This symmetric junction structure is likely to be a candidate for building sensors, microfludidices, electromechnical coupled devices and transducers,[14,15] optical component in microelectronic mechanic system and photovoltaics.[12]

The sponsorships from Research Grant Manpower Fund (RGM 21/04) of Nanyang Technological University, and Science and Engineering Research Council Grant No. (0421010010) from the Agency for Science, Technology and Research (A*STAR), Singapore are gratefully acknowledged. C.X.X. would like to acknowledge the financial support from the National Natural Science Foundation of China (60576008) and the Research Fund for Doctoral Program of Higher Education (20050286004).

[1] M. H. Huang, S. Mao, H. Feick, H. Yan, Y. Wu, H. Kind, E. Weber, R. Russo, and P. Yang, Science **292**, 1897 (2001).
[2] W. I. Park, D. H. Kim, S. W. Jung, and G. C. Yi, Appl. Phys. Lett. **82**, 4232 (2003).
[3] W. I. Park, G. C. Yi, M. Kim, and S. J. Pennycook, Adv. Mater. (Weinheim, Ger.) **14**, 1841 (2002).
[4] C. X. Xu and X. W. Sun, Appl. Phys. Lett. **83**, 3806 (2003).
[5] R. C. Wang, C. P. Lium, J. L. Huang, S. J. Chen, Y. K. Tseng, and S. C. Kung, Appl. Phys. Lett. **87**, 013110 (2005).
[6] J. J. Wu, S. C. Liu, C. T. Wu, K. H. Chen, and L. C. Chen, Appl. Phys. Lett. **81**, 1312 (2002).
[7] Z. L. Wang, Adv. Mater. (Weinheim, Ger.) **15**, 432 (2003).
[8] C. X. Xu, X. W. Sun, Z. L. Dong, and M. B. Yu, J. Cryst. Growth **270**, 498 (2004).
[9] C. X. Xu, X. W. Sun, Z. L. Dong, and M. B. Yu, Appl. Phys. Lett. **85**, 3878 (2004).
[10] C. X. Xu and X. W. Sun, J. Cryst. Growth **277**, 330 (2005).
[11] X. Y. Kong, Y. Ding, R. Yang, and Z. L. Wang, Science **303**, 1348 (2004).
[12] J. Y. Lao, J. G. Wen, and Z. F. Ren, Nano Lett. **2**, 1287 (2002).
[13] C. X. Xu, X. W. Sun, B. J. Chen, Z. L. Dong, M. B. Yu, X. H. Zhang, and S. J. Chua, Nanotechnology **16**, 70-13 (2005).
[14] P. X. Gao and Z. L. Wang, J. Phys. Chem. B **106**, 12653 (2002).
[15] P. X. Gao and Z. L. Wang, Appl. Phys. Lett. **84**, 2883 (2004).
[16] Z. Tian, J. A. Voigt, J. Liu, B. Mchenzie, M. J. Mcdermott, M. A. Rodriguez, H. Konishi, and H. Xu, Nat. Mater. **21**, 821 (2003).
[17] F. Li, Y. Ding, P. Gao, X. Xin, and Z. L. Wang, Angew. Chem. **116**, 5350 (2004).
[18] C. X. Xu, X. W. Sun, Z. L. Dong, and M. B. Yu, Appl. Phys. Lett. **85**, 3878 (2004).
[19] Mark Winter, WebElements Period Table, http://www.webelements.com
[20] C. X. Xu and X. W. Sun, Jpn. J. Appl. Phys., Part 1 **42**, 4949 (2003).
[21] J. Q. Hu, Q. Li, N. B. Wong, C. S. Lee, and S. T. Lee, Chem. Mater. **14**, 121 (2002).
[22] Y. H. Leung, A. B. Djurišić, J. Gao, M. H. Xie, and W. K. Chan, Chem. Phys. Lett. **385**, 155 (2004).
[23] S. Chen, Z. Fan, and D. L. Carroll, J. Phys. Chem. B **106**, 10777 (2002).
[24] K. Zou, X. Y. Qi, X. F. Duan, S. M. Zhou, and X. H. Zhang, Appl. Phys. Lett. **86**, 013103 (2005).
[25] Z. R. Dai, Z. W. Pan, and Z. L. Wang, J. Am. Chem. Soc. **124**, 8673 (2002).